JOURNAL OF
EMERGING INVESTIGATORS

Article

Assessing the accuracy and efficiency of simplified gridded ion thruster simulations

Mark Asmar[1], Derek Kuldinow[2]

[1] Bloomfield Hills High School, Bloomfield Township, Michigan

[2] Department of Aeronautics and Astronautics, Stanford University, Stanford, California

SUMMARY

Electric propulsion is a method of spacecraft propulsion, where thrust is generated by accelerating ionized gas using electric fields. It is an essential part of deep space mobility, being far more fuel and space efficient than combustion thrusters. Gridded ion thrusters are a common mean of achieving electric propulsion, utilizing multiple grids with a voltage difference to accelerate ions. Because electric propulsion mainly employs electrostatic forces, which are easily controlled, it is easier to simulate than chemical propulsion, which requires the determination of reaction rates, collisions and internal pressure forces. Thus, a large amount of electric propulsion research is conducted through simulations, iterating tests in order to optimize thruster designs. However, highly accurate simulations require large computational resources to mitigate numerical noise. Naturally, it would be useful to find any way to minimize computation times while still producing accurate data. To explore this concept, we created a particle-in-cell simulation which deliberately underresolves particle statistics to determine the effects on extensive and intensive metrics. We hypothesized that intrinsic values would still be accurate while extrinsic values would diverge greatly. We normalized the results by a reference value and quantitatively compared them to the experimental data, which showed that intensive properties like specific impulse and velocity retained high accuracy with low particle number. Our findings suggest that preliminary simulations could be run quickly with much lower particle counts before more technically demanding and comprehensive simulations are performed.

INTRODUCTION

With the rise in interest in commercial spacecraft in recent years, there has been a strong push for developing more efficient propulsion methods. Because of the vast distances inherent to space travel, it is critical to reduce the amount of fuel necessary for a mission in order to reduce costs and/or travel time. The primary focus of current work on high-efficiency space propulsion is ion thrusters, which are found on a vast majority of space systems today due to their high specific impulse and small thruster size (1). Ion thrusters operate by first ionizing particles of a substance, typically a noble gas, and then accelerating the charged particles out of the spacecraft, generating thrust (1). Simulations play a crucial role in electric propulsion development, allowing researchers to test new ideas inexpensively and conveniently, such as different configurations or alternative fuels, before conducting real-world experiments.

There are a number of methods for simulating ion thrusters, with the most notable being particle-in-cell (PIC), fluid, and hybrid models (2). PIC offers the highest fidelity by capturing the motions of individual particles within the ionized gas, but can be computationally expensive due to the large number of particles required to recover accurate physics (3). Alternatively, fluid models treat the plasma as a continuous fluid, reducing computational requirements (3). However, fluid models only allow us to capture average quantities like density, bulk velocity, and temperature under the assumption that the plasma is sufficiently collisional to be near thermodynamic equilibrium (3). Hybrid models combine the two, generally treating ions as particles and electrons as a fluid or decomposing the domain into fluid-like and particle-like regimes, depending on the density and collisionality of the region of space (3).

Ideally, we would use PIC whenever feasible, especially when we want to study the thruster's plume where densities are low and collisions may not be numerous enough to bring the plasma to equilibrium. However, computational power can quickly become a limiting factor in these kinetic simulations. Previous work in this field has studied and compared the strengths and limitations of different simulation methods (3). The authors found that when simulating electrons with PIC, it takes over 1,000 macroparticles per cell in order to minimize numerical heating, which is the erroneous increase or decrease of particle velocity as a consequence of noise in the simulation (3). It is essential to reduce numerical heating to ensure velocities are appropriately represented and not overestimated. However, 1,000 macroparticles per cell can be translated to hundreds of millions of particles in a moderately sized simulation. Even lower fidelity simulations still require hundreds of particles per cell. This issue can be mitigated in simulations focused on ion extraction and optics by treating electrons as a fluid. Meanwhile, it is identified that at least 40 ion macroparticles per cell are required to avoid significant numerical noise; this is much lower than what is needed for electrons but can still lead to long computation times (4).

To address those challenges, we sought to determine how simplified ion thruster simulations compare to existing data in terms of accuracy and computational efficiency. We hypothesized that running a simulation with insufficient particle counts would lead to inaccurate extrinsic measurements but would still produce accurate results for intrinsic properties. We measured extrinsic values such as thrust, mass flow rate

https://doi.org/10.59720/24-381

of particles leaving the thruster, and the plume density of said particles at a distance outside of the thruster. We also measured the following intrinsic values: max and average horizontal exit velocity of propellants, specific impulse, average particle exit angle (plume angle), and impingement, the rate of particles that collide with the thruster geometry. We found that said intrinsic values remained mostly accurate despite the lower fidelity of the simulation, suggesting that faster, lower precision simulations could be run to capture these values before moving to high fidelity simulations.

RESULTS

We ran simulations with a PIC code, all with the same gridded ion thruster geometry, modeled from the QinetiQ T5 thruster with the dimensions supplied from Fazio, et al. 2018 (5). We simplified the 3D thruster space onto an RZ plane with the assumption of axial symmetry, which spans from the inside of the thruster to 1 cm into the plume. We simulated thrusters that use the following seven propellants as the working gas: xenon, krypton, argon, neon, helium, hydrogen, and iodine. We simulated each of these propellants three times and averaged their results.

From the unaltered simulation results, we saw a large discrepancy between our simulated specific impulse and the specific impulse in our chosen literature (5). This is because our simulation calculated specific impulse solely based on ionized particles that leave the thruster, while Fazio, et al. considers specific impulse in the context of all of the propellent (5). Thus, we adjusted our specific impulse by multiplying it with the mass utilization ratio $\eta_m \approx 0.865$ (**Table 1**). We found that the error between our corrected Isp and that presented in Fazio, et al. is at most 5.33% (**Figure 1 and Table 2**).

As expected, plume density was subject to variation due to significant noise in between time steps. The propellant with the most variation was hydrogen, with an average plume density of 4.71E+11 particles/m^3 and standard deviation of 3.89E+11 particles/m^3. Plume density is correlated with thrust. Even though our values for absolute plume density would be inaccurate, it was useful to compare the relative plume densities among propellants. Iodine presented the highest plume density out of all the propellants, followed by xenon and then krypton. Meanwhile, argon had around half of the plume density of xenon, but is significantly cheaper (**Table 2**). All of the propellants we evaluated had very similar divergence angles, with hydrogen having the smallest at 11.6°, and krypton the greatest at 13.65°. However, individual results are susceptible to numerical noise since the value is an aggregate of the last ten time steps. Despite this, repeated measurements were all within 1° of each other. The small range of values between different propellants can be explained since the divergence angle is a ratio between the r and z velocities, which is in turn directly related to the r and z electric fields. Therefore, while heavier propellants might have a smaller charge to mass ratio, it ultimately would not affect the ratio in velocities.

Another statistic that was consistent was grid impingement, with all propellants incurring between 14 and 16% impingement. Because of this consistency, we drew a relationship between grid erosion and propellant mass. Lighter propellants need more individual particles, which all carry approximately the same energy no matter the mass. Since they are accelerated through the same potential, the lighter propellants would have more total energy colliding with the grid (**Table 2**).

Although the massively decreased ion production rate would result in equally incorrect mass flow rates, we still found it important to ensure that the mass flow rates were internally consistent. To observe this, we normalized the mass flow rate relative to xenon before comparing to literature values. We found that our values closely matched those from literature once normalized (**Figure 2**).

Finally, average velocity was very accurate across all propellants, with the greatest error being 2.38%, showing that even without meeting the threshold of 40 particles per cell, this value remains consistent (**Table 2 and Figure 3**). Additionally, while maximum particle velocity remained relatively close to average velocity for most propellants, the maximum velocity for hydrogen was considerably higher than its average velocity (**Table 2**).

Propellant	Xe	Kr	Ar	Ne	He	H_2	I
M_i (amu)	131.3	83.8	39.9	20.2	4	2	126.9
I_b (mA)	457	572	829	1,166	2,618	3,689	465
v_i (m/s)	40,209	50,330	72,895	102,563	230,290	324,490	40,889
$\dot{m}_i$ (mg/s)	0.622	0.497	0.343	0.244	0.109	0.077	0.611
T_{corr} (mN)	23.71	23.71	23.71	23.71	23.71	23.71	23.71
I_{sp} (s)	3,359	4,205	6,090	8,569	19,241	27,111	3,417
η_m	0.864	0.864	0.864	0.865	0.865	0.865	0.863

Table 1: Plume and thrust characteristics for various propellants in gridded ion thrusters from Fazio, et al. (5). The value η_m represents the mass utilization ratio, and is calculated from experimental results.

DISCUSSION

Overall, our results were surprisingly accurate and consistent despite the low fidelity of the simulation. While the values obtained from our simulations for mass flow rate were significantly lower than the experimental data in the literature, this can be explained by an inaccurate input value for ion production rate (5). As a consequence of

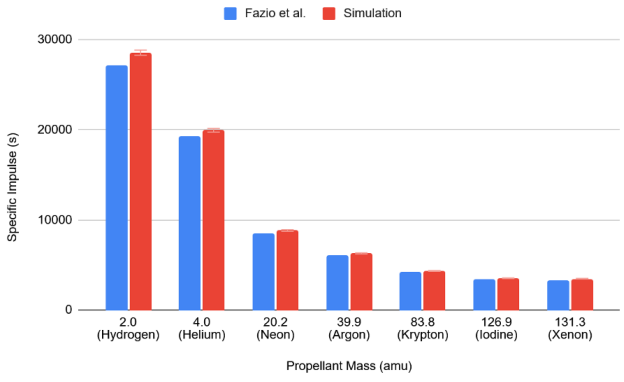

Figure 1: Specific impulse at varying propellant masses. Simulation results (red, n=3) compared to literature values (blue, from Fazio et al. (5)). Error bars represent three standard deviations of the highest variation for specific impulse among all the propellants (equivalent to 1%). Specific impulse was measured by dividing the average exit velocity by the acceleration of gravity on Earth (9.81 m/s^2).

https://doi.org/10.59720/24-381

Propellant	Xe	Kr	Ar	Ne	He	H_2	I
Plume Density (particles/m³)	3.76E+12	3.54E+12	1.68E+12	9.28E+11	7.48E+11	3.06E+11	4.68E+12
Max Z-Velocity (m/s)	41,575	51,942	75,077	105,779	240,863	445,163	42,146
Average Horizontal Exit Velocity (m/s)	39,469	49,210	71,436	100,121	222,962	323,786	40,096
Average Plume Angle (°)	13.17	13.65	13.23	13.49	12.6	11.6	13.3
Average I_{sp} (s)	4,023	5,016	7,282	10,206	22,728	33,006	4,087
Impingement (%)	14.77	14.51	15.02	14.84	15.49	14.38	14.64
$\dot{m}_i$ (mg/s)	2.54E-04	1.90E-04	6.22E-05	2.48E-05	9.17E-06	2.33E-06	3.11E-04
Thrust (mN)	1.00E-02	9.36E-03	4.44E-03	2.48E-03	2.04E-03	7.56E-04	1.25E-02
Expected ṁ/Actual	2.45E+03	2.61E+03	5.51E+03	9.83E+03	1.19E+04	3.30E+04	1.96E+03
Expected T/Actual	2.36E+03	2.53E+03	5.34E+03	9.54E+03	1.16E+04	3.14E+04	1.90E+03
Adjusted I_{sp} % Error	3.47	3.23	3.11	3.31	3.05	2.19	5.33
Velocity % Error	1.84	2.23	2.00	2.38	3.18	0.22	1.94

Table 2: Plume and thrust characteristics for various propellants in a gridded ion thruster as measured in our Particle-In-Cell simulation. Mass flow rate and thrust are calculated from velocity, ion mass, and plume density as found in this table; their calculations are shown in the methods section **(Equations 4 and 5).** The value ṁ represents mass flow rate. Impingement is measured as the percent of particles that collided with thruster geometry over all particles that collided with or successfully exited the thruster.

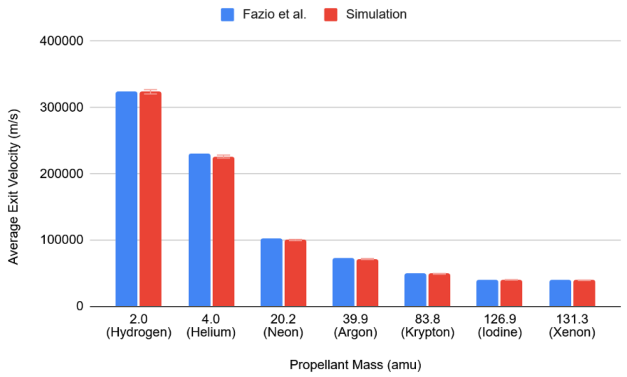

Figure 2: Mass flow rate versus propellant mass, normalized by the mass flow rate of Xenon. Simulation results (red, n=3) compared to literature values (blue, from Fazio et al. (5)). Error bars represent three standard deviations of the highest variation for specific impulse among all the propellants (equivalent to 1%). Mass flow rate was calculated as presented in equation 4. All values were normalized by dividing them by the mass flow rate for Xenon.

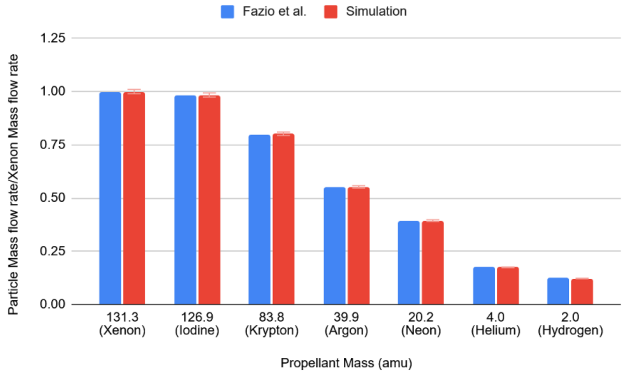

Figure 3: Average propellant horizontal exit velocity to propellant mass. Simulation results (red, n=3) compared to literature values (blue, from Fazio et al. (5)). Error bars represent three standard deviations of the highest variation for average exit velocity among all the propellants (equivalent to 1%). Average exit velocity was calculated by averaging the horizontal velocities of particles as they exit the thruster.

computational limits, the combination of specific weight and ion production rate leads to fewer than 10 macroparticles per cell in certain regions of the simulation domain, lower than the recommended 40 macroparticles per cell for smooth statistics. Achieving higher ion production rate while aligning with our goal of analyzing reduced macroparticle counts would require a substantially higher specific weight; however, increasing the specific weight too much would result in effectively heavy point charges wherein single particles can significantly affect the electric field profiles, resulting in unreliable data. Although operating at a significantly lower mass production rate leads to unrealistic results, we believe that by focusing on resolving the measurements of interest, we can yield more useful and specific results.

Even when lacking the complexities of a typical simulation, our simulation was able to accurately predict intrinsic values like average velocity and specific impulse with a difference within 6% when compared to experimental data from literature, particularly for heavier propellants (5). This opens the door to running smaller preliminary simulations of full-sized thrusters before switching to comprehensive simulation. Although average velocity was consistent, max velocity was prone to error for the lighter propellants, especially hydrogen. This is likely because as the lightest propellant, hydrogen has high velocities and is thus more prone to spontaneous heating as a result of insufficient grid fidelity, suggesting that precision must still be respected as particle speed increases. More rigorous spatial and temporal convergence studies should be performed in future simulations to yield more accurate results.

We found that iodine has the highest plume density. While this could make it a cheaper alternative to xenon, its high reactivity makes it difficult to use. The next most commonly considered alternative to xenon is argon, which despite having a much higher ionization energy and about half of the plume density, is prized for its significantly lower costs (5). Meanwhile, krypton had a close density to xenon while having about a quarter of the price, at the expense of a slightly higher ionization energy (5). This suggests that krypton could make for a prospective substitute when we balance cost and efficiency, though more analysis still needs to be done.

It was difficult to capture extensive properties like thrust and space charge limiting factors due to insufficient ion production rate. These values were also particularly sensitive to noise, likely because of insufficient particle counts, with values such as plume density having large standard deviations that are, at worst, almost equal to the mean. Future researchers with access to greater computational resources could repeat our work with finer resolution in both space and time to quantify

https://doi.org/10.59720/24-381

how the error decreases with increased fidelity. With better optimizations, the framework presented in this study has the potential to be a good starting ground for testing new ideas at the scale of a full thruster instead of being restricted to a limited amount of individual apertures. Furthermore, the dimensions utilized in the simulation are most likely different from those in experiment. With access to proprietary designs and data, the simulation could be compared to experimental data for a more accurate analysis.

MATERIALS AND METHODS

Computer specifications

For this simulation, we used a computer with an AMD Ryzen 5 2400G for the processor, a Radeon RX 580 (4 GB) for the graphics card, and 16 GB of memory.

Simulation methodology

Because details of the thruster geometry are proprietary, not all of the thruster measurements are available, meaning we had to approximate some of the dimensions based on realistic design. Additionally, the grid resolution was not fine enough to exactly match experimental specifications, so all spatial measurements were rounded to the nearest 0.25 mm. The parameters used in the simulations are listed below (**Table 3**). Parameters marked with an asterisk (*) indicate values required for this study, but that were not reported in the literature, so we chose appropriate numerical values (5). Measurements of the acceleration grid were chosen since acceleration grids are almost always thicker than screen grids and have smaller aperture sizes (6). Meanwhile, the value for ion production rate was selected to limit computational times and problems that arise from high specific weights. Although many specific measurements are proprietary, a schematic of the T5 Thruster was depicted at the 8th international European Space Agency conference (7). We noted that the axisymmetric assumption increases grid transparency because the grid is effectively replaced by annular holes.

Physical Parameter	Value in Simulations	Physical Parameter	Value in Simulations
Cell Width (mm)	0.25	Screen Grid Voltage (V)	1,060
Thruster Radius (cm)	5	Accel Grid Voltage (V)	-225
Grid Gap l_g (mm)	0.75	Inner Tube Length (mm)	15
Screen Grid Thickness (mm)	0.25	Ion Production Rate (s^{-1})	1.6E18 *
Screen Grid Aperture Radius (mm)	1.00 (rounded from 1.07)	Specific Weight	5E+4
Screen Grid Spacing	1 mm*	Timestep Size (s)	5E-9
Accel Grid Thickness (mm)	0.50*	Z-nodes (Nz)	100
Accel Grid Aperture Radius (mm)	0.75*	R-nodes (Nr)	215
Accel Grid Spacing (mm)	1.50*		

Table 3: Constant parameters used in the simulation. Values marked with an asterisk (*) represent data not reported in literature that we approximated based on realistic thruster design. The reasoning for these values is explained in simulation methodology.

Our simulations were adapted from open-source code for a hybrid model ion gun from the Particle-in-Cell blog by Lubos Brieda, which treats ions as particles while electron density is calculated by assuming a Boltzmann distribution (8). The simulation assumed that the maximum density of the electrons is equal to the maximum density of the ions at the potential of the acceleration grid. The electron density at all other positions was determined by assuming a temperature of 5 eV and a Boltzmann distribution. The simulation employed a 2D axisymmetric geometry in space. Velocities were treated in full 3D, and particles were rotated back into the simulation plane every timestep to gather density for electric potential calculations. This allowed for a simpler simulation while preserving realistic movement under the assumption of axial symmetry. For calculating the spatial ion density at the grid nodes, particle weights were linearly interpolated to the four corners of their cell. This interpolation of ion density, combined with the Boltzmann distribution for electrons, was used to determine the charge density in Poisson's equation for electrostatic potential. The potential structure was calculated using Poisson's equation in cylindrical coordinates:

$$\frac{\partial^2\phi}{\partial r^2}+\frac{1}{r}\frac{\partial\phi}{\partial r}+\frac{1}{r^2}\frac{\partial^2\phi}{\partial\theta^2}+\frac{\partial^2\phi}{\partial z^2}=-\frac{\rho}{\epsilon_0} \quad \textbf{(Equation 1)}$$

where φ is electrostatic potential [V], ρ is charge density [C/m3], and ε_0 is the vacuum permittivity of space. The third term is dropped under the assumption of axial symmetry, then the equation was discretized for the simulation (**Equation 2**). Then, the equation was rearranged to solve for φ (**Equation 3**).

$$\frac{\phi_{i,j+1}-2\phi_{i,j}+\phi_{i,j-1}}{(\Delta r)^2}+\frac{1}{r_{i,j}}\frac{\phi_{i,j+1}-\phi_{i,j-1}}{2\Delta r}+\frac{\phi_{i-1,j}-2\phi_{i,j}+\phi_{i+1,j}}{(\Delta z)^2}=-\frac{\rho}{\epsilon_0} \quad \textbf{(Equation 2)}$$

$$\phi_{i,j}=\left[\frac{\rho}{\epsilon_0}+\frac{\phi_{i,j+1}+\phi_{i,j-1}}{(\Delta r)^2}+\frac{1}{r_{i,j}}\frac{\phi_{i,j+1}-\phi_{i,j-1}}{2\Delta r}+\frac{\phi_{i-1,j}+\phi_{i+1,j}}{(\Delta z)^2}\right]/\left(\frac{2}{\Delta r^2}+\frac{2}{\Delta z^2}\right) \quad \textbf{(Equation 3)}$$

In the simulation, this was resolved with a Jacobian Solver that iteratively computed the finite difference between cells to approximate the field.

The electric field was calculated by taking the difference in potential between two nodes and dividing by distance. Finally, particles were pushed by the electric field by linearly interpolating the electric field from the cell nodes to the particle position. The simulation did not consider collisions between particles, and when particles were pushed out of the simulation boundaries, they were removed from the simulation.

The ion production rate was a product of the chosen neutral production rate, electron production rate, and a coefficient for the rate of successful ionizations, which in the simulation was 10^{15}, 10^{12}, and 1.6E-7, respectively. Note that these individual values held no use in the simulation outside of the initial calculation for ion production rate. Every time step, particles were injected into the assigned cells based on this production rate, with any remaining fractional particles being contributed to the next time step. Particles in this simulation were macroparticles, representing thousands of physical particles with one simulated particle. The amount of real particles represented by one macroparticle is known as

https://doi.org/10.59720/24-381

the specific weight.

Most of the data we presented was measured in simulation, however some were calculated afterwards using simulation results equations (**Table 2**). These values were calculated through the following equations.

Mass flow rate is calculated as:

$$\dot{m} = \rho v M \pi r^2 \qquad \textbf{(Equation 4)}$$

where $\dot{m}$ is mass flow rate (kg/s), ρ is plume density (particles/m^3), v is average ion horizontal exit velocity, M is ion mass, and r is the radius of the thruster. Plume density is calculated by averaging the cell densities from the exit plane, while velocity is calculated by averaging the velocity of particles as they leave the thruster.

Thrust is calculated as:

$$T = \dot{m} v \qquad \textbf{(Equation 5)}$$

where T is thrust (N), $\dot{m}$ is mass flow rate and v is average ion horizontal exit velocity.

Most of results presented by Fazio, et al. were calculated in ways that are consistent with our methods, however specific impulse was a notable exception since we measured it directly in simulation. Specific impulse is calculated by Fazio, et al. as:

$$I_{sp} = \frac{\gamma \eta_m}{g} \sqrt{\frac{2eV_b}{M}} \qquad \textbf{(Equation 6)}$$

where γ is the thrust correction factor, g is the acceleration of gravity (9.807 m/s^2), $\eta_m = \dot{m}_i / \dot{m}_p$ is the thruster mass utilization efficiency (with $\dot{m}_i$ being ion mass flow rate and $\dot{m}_p$ being total mass propellant flow rate), V_b is beam voltage, (the net voltage through which the ion is accelerated), e is the electron charge, and M is the ion mass (kg) (5). The thrust correction factor is a coefficient used to account for beam divergence and multiple charged species and is valued at 0.948 for the T5 thruster (5).

Received: December 19, 2024
Accepted: May 2, 2025
Published: January 13, 2026

REFERENCES

1. Holste, Kristof, et al. "Ion thrusters for electric propulsion: Scientific issues developing a niche technology into a game changer." *Review of Scientific Instruments*, vol. 91, no.6, 2020. https://doi.org/10.1063/5.0010134
2. Colonna, Gianpiero, and Antonio D'Angola. *Plasma Modeling: Methods and Applications.* IOP Publishing, 2nd ed., pp. (4-5) & (6-1) 2022. https://doi.org/10.1088/978-0-7503-3559-1
3. Kim, H. C., et al. "Particle and fluid simulations of low-temperature plasma discharges: benchmarks and kinetic effects." *Journal of Physics D: Applied Physics* 38.19 (2005): R283. https://doi.org/10.1088/0022-3727/38/19/R01
4. Garrigues, Laurent, et al. "Appropriate use of the particle-in-cell method in low temperature plasmas: Application to the simulation of negative ion extraction." *Journal of Applied Physics* 120.21 (2016). https://doi.org/10.1063/1.4971265
5. Fazio, Nazareno, et al. "Alternative propellants for gridded ion engines." (2018): SP2018_00102. http://eprints.soton.ac.uk/id/eprint/422369
6. Laya, Neil P., and Kunning G. Xu. "Optimization of Screen Grid Aperture Diameter and Aperture Count in Ion Thrusters for Maximum Screen Grid Ion Transparency." *AIAA SCITECH 2022 Forum*. 2022. https://doi.org/10.2514/6.2022-1562
7. Romanazzo, Massimo, et al. "In-orbit experience with the drag-free attitude and orbit control system of ESA's gravity Mission GOCE." 8th International ESA Conference on Guidance, Navigation & Control Systems. 2011.
8. Brieda, L. (2015, June 15). Particle in cell method in cylindrical coordinates. www.particleincell.com. www.particleincell.com/2015/rz-pic